A Fractional-Order Sliding Mode Controller Design for Cable-Driven Parallel Robots

Hamzeh Ansari[1*], and Mostafa Siavashi[2]

Abstract: **In this paper, the fractional-order sliding mode approach is employed to control a cable-driven parallel robot. Due to uncertainties in kinematic and dynamic parameters, as well as the use of tension cables, cable-driven robots inherently exhibit a vibrating structure and uncertainty. Consequently, robustness is a crucial aspect of controlling such systems. To achieve full controllability, actuation redundancy is also necessary. For all cable-driven robots, the cables cannot have negative tension values. Furthermore, because of the positive tension in the cables, the control rules must also yield positive values. The combination of positive tension, actuation redundancy, and a vibrating structure makes the control of these robots a challenging problem for engineers, highlighting the importance of designing a robust controller. In this article, robust sliding mode controllers are modified using the fractional-order approach. The proposed method demonstrates superior results compared to the conventional sliding mode method, particularly under disturbance conditions. The Lyapunov stability theorem is utilized to establish the stability and validity of the proposed method, and its effectiveness is illustrated through simulations in MATLAB/Simulink.**

Keywords: **Cable driven parallel robot, Fractional-order, Sliding mode controller, Stability.**

I Introduction

Today, simple cable robots and cable-driven parallel robots (CDPRs) are prominent examples of robots used in engineering and industrial applications. For instance, these specialized robots are employed in monitoring aquatic environments, simulator devices, contour crafting systems [1], 3D printing devices [2], virtual training devices [3], and more. Consequently, CDPRs have been increasingly explored from various perspectives and approaches.

A Literature

The primary issues examined in this literature include the kinematics, dynamics, and control of CDPRs. Additionally, one of the key elements in these studies is the cables utilized in CDPRs. The adoption of flexible cables in CDPRs, as opposed to rigid links, offers significant advantages such as a high payload-to-weight ratio, high-speed motion, low production costs, and expansive workspaces [4]. Furthermore, CDPRs can be easily reconfigured and implemented [5]. However, the elastic properties of the flexible cables can potentially lead to unwanted motions of the end-effector, resulting in errors in its orientation and position. Thus, the use of flexible cables in CDPRs introduces new challenges and drawbacks in their control. In other words, precisely controlling the end effector in CDPRs presents a challenging problem. To address this issue, various research efforts have been undertaken to design effective controllers for CDPRs. Consequently, a range of strategies has been proposed for controlling CDPRs. For example, in [6], a Lyapunov-based technique was introduced to effectively control a cable-suspended robot. In [7], a robust sliding mode control strategy for a 6-DOF cable-suspended parallel robot under uncertain disturbances was presented. Taghirad *et al.* proposed a robust PID controller for fully-constrained CDPRs [8]. Khosravi *et al.* developed a dynamic model for a CDPR and subsequently designed a sliding mode controller, identifying chattering as the primary issue with their controller [9]. Babaghasabha *et al.* created an adaptive robust sliding mode controller by adapting the upper bound of the uncertainties [10]. Additionally, Babaghasabha *et al.* designed and implemented an adaptive controller for a cable-driven robot named KNTU, addressing uncertainties in dynamic and kinematic parameters. Generally, CDPRs can be categorized into two types: 2D (or planar) CDPRs and 3D CDPRs. An empirical study on a planar CDPR utilizing robust PID control was presented in [11]. Oh *et al.* developed a control strategy based on positive tension controllers for a planar CDPR with redundant cables [12]. A model-predictive controller was created for a 3D CDPR [13]. Furthermore, experimental work has been conducted on CDPRs to validate the effectiveness of various control strategies. For instance, Xue *et al.* employed a feed-forward controller to reduce tracking position errors in a laparoscopic surgical robot [14]. In another experimental study, Bayani *et al.* designed a vision-based position controller for a planar CDPR [15]. The four-bar linkage kinematic concept was utilized for the kinematic modeling of the robot. They also developed a technique based on the Recursive Least Squares algorithm to mitigate uncertainties in the parameters of the kinematic model. For developing a robotic system, especially CDPRs, modeling uncertainties are a major problem [16]. Kinematic and dynamic uncertainty modeling of CDPRs, as well as the effects of parameter uncertainties in

[1] Farazgaman Company, Shariati Street, Tehran, 63135-16116, Iran
[2] Farazgaman Company, Shariati Street, Tehran, 63135-16116, Iran
* Corresponding Author, Email: hamzeh_ansari@yahoo.com

the kinematic and dynamic models, have been the focus of many studies. For instance, Babaghasabha *et al.* proposed an adaptive robust sliding mode controller based on adaptation of the upper bound of the uncertainties [9]. Korayem *et al.* [17] designed a sliding mode controller for a cable-suspended robot to compensate for flexibility uncertainties. Indeed, disturbance and uncertainty are the main challenges in modeling and control of CDPRs. Usually, disturbances originate from the robot's environment [18,19], arising from noise, variations, and set-point changes. Under external disturbances, the end-effector may experience large horizontal sway and oscillations, especially when the end-effector is light in CDPRs [20]. To overcome this, various studies have been performed. For example, in [11] a robust sliding mode control approach under uncertain disturbances was applied to a 6-DOF cable-suspended parallel robot.

B Contribution

In this paper, we also use a robust sliding mode control approach to address uncertainty and disturbance. When compared to traditional control methods, sliding mode control stands out due to its straightforward implementation, strong robustness against system uncertainties, and notably rapid transient performance [21,22]. Here, we modify the traditional sliding mode control using fractional calculus mathematics and compare the performance of the traditional sliding mode controller with our proposed fractional-order (FO) sliding mode approach under varying gain parameters. The performance of the two controllers is studied under disturbance conditions, and the Lyapunov stability theorem is used to prove the stability and validity of the proposed method. Simulations in MATLAB/Simulink are used to demonstrate the effectiveness of the proposed method.

C Organization

The rest of this paper is organized as follows. In Section II, the kinematics and dynamics of cable-driven parallel robots are examined. In Section III, a simple sliding mode controller is designed. Section IV presents a novel FO sliding mode controller for the cable-driven parallel robot. Then, in Section V, the performance of the integer-order sliding mode controller is compared with that of the designed controller. Finally, Section VI concludes and suggests directions for future work.

II Modeling

Assuming negligible cable mass and flexibility, the motion equation of the cable-driven parallel robot can be expressed as

$$M(X)\ddot{X} + h(X,\dot{X}) = -J^T(X)\tau \tag{1}$$

where

$$h(X,\dot{X}) = C(X,\dot{X})\dot{X} + G(X) + N(\dot{X}) + T_d \tag{2}$$

and

$$N(\dot{X}) = F_d(\dot{X}) + F_s(\dot{X}) \tag{3}$$

Here, X denotes the generalized coordinate vector of the end-effector, $M(X)$ is the positive-definite inertia matrix, $C(X,\dot{X})$ represents the Coriolis and centrifugal terms, $G(X)$ denotes the gravitational force vector, $N(\dot{X})$ represents the friction force, T_d denotes the external disturbance, τ is the cable tension vector, and $J(X)$ is the configuration-dependent Jacobian matrix. The generalized coordinate vector of the planar CDPR is given by

$$X = \begin{bmatrix} x & y & \phi \end{bmatrix}^T \in \mathbb{R}^3 \tag{4}$$

On the other hand, the actuator dynamics are expressed as [23]

$$I_m\ddot{q} + D\dot{q} - r\tau = u \tag{5}$$

where $q \in \mathbb{R}^4$ is the actuator shaft-angle vector, I_m is the actuator inertia matrix, D is the viscous damping matrix, r is the drum radius, $u \in \mathbb{R}^4$ is the actuator torque vector, and $\tau \in \mathbb{R}^4$ is the cable tension vector.

The cable-length variation is given by

$$\Delta L = rq = L - L_0 \tag{6}$$

which leads to

$$q = r^{-1}(L - L_0) \tag{7}$$

The cable-length velocity is related to the end-effector velocity through

$$\dot{L} = J(X)\dot{X} \tag{8}$$

Therefore,

$$\dot{q} = r^{-1}J(X)\dot{X} \tag{9}$$

Since the Jacobian matrix is generally configuration-dependent, its time derivative cannot, in general, be neglected. Hence, differentiating (9) yields

$$\ddot{q} = r^{-1}J(X)\ddot{X} + r^{-1}\dot{J}(X,\dot{X})\dot{X} \tag{10}$$

where

$$\dot{J}(X,\dot{X}) = \frac{\partial J(X)}{\partial X}\dot{X} \tag{11}$$

Substituting (9) and (10) into (5) gives

$$\begin{aligned} I_m\left[r^{-1}J(X)\ddot{X} + r^{-1}\dot{J}(X,\dot{X})\dot{X}\right] \\ + Dr^{-1}J(X)\dot{X} - r\tau = u \end{aligned} \tag{12}$$

Consequently, the cable tension vector is obtained as

$$\begin{aligned} \tau = r^{-1}\Big[& I_m r^{-1}J(X)\ddot{X} + I_m r^{-1}\dot{J}(X,\dot{X})\dot{X} \\ & + Dr^{-1}J(X)\dot{X} - u\Big] \end{aligned} \tag{13}$$

Substituting (13) into (1), and multiplying the resulting equation by r, yields the equivalent dynamic model

$$M_{eq}(X)\ddot{X} + h_{eq}(X,\dot{X}) = J^T(X)u \tag{14}$$

where

$$M_{eq}(X) = rM(X) + J^T(X)I_m r^{-1}J(X) \tag{15}$$

and

$$\begin{aligned} h_{eq}(X,\dot{X}) = {} & rh(X,\dot{X}) \\ & + J^T(X)I_m r^{-1}\dot{J}(X,\dot{X})\dot{X} \\ & + J^T(X)Dr^{-1}J(X)\dot{X} \end{aligned} \tag{16}$$

Accordingly, the equivalent dynamics can be written in the following MIMO state-space form:

$$\ddot{X} = f(X, \dot{X}) + g(X)u \tag{17}$$

where

$$f(X, \dot{X}) = -M_{\text{eq}}^{-1}(X)h_{\text{eq}}(X, \dot{X}) \tag{18}$$

$$g(X) = M_{\text{eq}}^{-1}(X)J^T(X) \tag{19}$$

Therefore, we have

$$\ddot{X} = -M_{\text{eq}}^{-1}(X)h_{\text{eq}}(X, \dot{X}) + M_{\text{eq}}^{-1}(X)J^T(X)u \tag{20}$$

Since the considered CDPR is redundantly actuated, a virtual task-space control input $v \in \mathbb{R}^3$ is introduced. The actuator control input is allocated as

$$u = \left(J^T(X)\right)^{\dagger} v + N(J^T(X))\eta \tag{21}$$

where

$$N(J^T(X)) = I_4 - \left(J^T(X)\right)^{\dagger} J^T(X) \tag{22}$$

is the null-space projector and $\eta \in \mathbb{R}^4$ is an arbitrary redundancy-resolution vector.

Since

$$J^T(X)N(J^T(X)) = 0 \tag{23}$$

it follows that

$$J^T(X)u = v \tag{24}$$

(14) can be also rewritten as

$$\ddot{X} = f(X, \dot{X}) + b(X)v \tag{25}$$

where

$$b(X) = M_{\text{eq}}^{-1}(X) \tag{26}$$

The redundancy-resolution vector η should be selected such that the physical cable-tension constraints are satisfied:

$$\tau_i(t) \geq 0, \qquad i = 1, \dots, 4 \tag{27}$$

In the considered operating region, the Jacobian matrix is approximated by a constant numerical matrix evaluated at the nominal configuration. Accordingly, its time derivative is assumed to be zero, i.e., $\dot{J} = 0$, and all subsequent modeling and control-design derivations are developed under this assumption.

III Controller Design

One major disadvantage of simple sliding mode controllers is the chattering phenomenon. Chattering produces high-frequency, small-amplitude oscillations that cause thermal losses in power circuits and mechanical wear. In robotic systems, chattering often arises from unmodeled uncertainties. Although conventional sliding mode controllers cannot completely eliminate chattering, its side effects can be reduced using other techniques. Two main factors contribute to chattering: the presence of the sign function and the gain applied to it in the control input. Many approaches have been proposed to mitigate chattering, such as higher-order sliding mode. In this study, the FO sliding mode controller is adopted to address the problem. The next section describes the controller design process for the CDPR.

The tracking error vector is defined as

$$e(t) = X_d(t) - X(t) \tag{28}$$

where $X_d(t)$ denotes the desired trajectory.

The FO sliding surface is defined as

$$s(t) = {}^{C}D_t^{\alpha} e(t) + \Lambda e(t), \qquad 0 < \alpha < 1 \tag{29}$$

where ${}^{C}D_t^{\alpha}$ denotes the Caputo fractional derivative of order α, and

$$\Lambda = \Lambda^T > 0 \tag{30}$$

To explicitly account for modeling uncertainties and external disturbances, the system dynamics are represented as

$$\ddot{X} = \hat{f}(X, \dot{X}) + \hat{b}(X)v + \Delta(X, \dot{X}, t) \tag{31}$$

where $\hat{f}(X, \dot{X})$ and $\hat{b}(X)$ denote the estimated dynamics and input matrix, respectively, and $\Delta(X, \dot{X}, t)$ represents the lumped modeling uncertainty and external disturbance. It is assumed that

$$\left\|\Delta(X, \dot{X}, t)\right\| \leq \Delta_{\max} \tag{32}$$

The equivalent control is selected as

$$v_{\text{eq}} = \hat{b}^{-1}(X) \left[\ddot{X}_d - \hat{f}(X, \dot{X}) + {}^{C}D_t^{1-\alpha} \Lambda \dot{e}\right] \tag{33}$$

The switching control is defined as

$$v_{\text{sw}} = K_{\text{sm}} \operatorname{sgn}(s) \tag{34}$$

where $K_{\text{sm}} = K_{\text{sm}}^T > 0$. Therefore, the virtual control law is selected as

$$\begin{aligned} v = \hat{b}^{-1}(X)\Big[&\ddot{X}_d - \hat{f}(X, \dot{X}) \\ &+ {}^{C}D_t^{1-\alpha} \Lambda \dot{e} + K_{\text{sm}} \operatorname{sgn}(s)\Big] \end{aligned} \tag{35}$$

Finally, the corresponding actuator input is obtained through the redundant control allocation

$$u = \left(J^T(X)\right)^{\dagger} v + N(J^T(X))\eta \tag{36}$$

Consider the following Lyapunov function:

$$V(t) = \frac{1}{2} s^T(t)s(t) \tag{37}$$

Taking the time derivative of (37) gives

$$\dot{V}(t) = s^T(t)\dot{s}(t) \tag{38}$$

Under the proposed control law, the sliding-variable dynamics are represented as

$$\dot{s} = -K_{\text{sm}} \operatorname{sgn}(s) + \Delta_s \tag{39}$$

where Δ_s represents the lumped uncertainty in the sliding-variable dynamics and satisfies

$$\|\Delta_s\| \leq \Delta_{\max} \tag{40}$$

Substituting (39) into (38) yields

$$\dot{V} = s^T \left[-K_{\rm sm}\,\mathrm{sgn}(s) + \Delta_s\right] \tag{41}$$

Using the uncertainty bound, it follows that

$$\dot{V} \leq -\lambda_{\min}(K_{\rm sm})\,\|s\|_1 + \Delta_{\max}\,\|s\| \tag{42}$$

If the switching gain is selected such that

$$\lambda_{\min}(K_{\rm sm}) > \Delta_{\max} + \eta, \qquad \eta > 0 \tag{43}$$

then

$$\dot{V} \leq -\eta\,\|s\| < 0, \qquad s \neq 0 \tag{44}$$

Therefore, the reaching condition is satisfied and the sliding variable converges to the sliding manifold:

$$s(t) \to 0 \tag{45}$$

Once the sliding manifold is reached,

$$s(t) = 0 \tag{46}$$

the reduced-order error dynamics are obtained as

$${}^{C}D_t^{\alpha} e(t) = -\Lambda e(t) \tag{47}$$

From [24], we can conclude that the FO sliding dynamics are asymptotically stable if all eigenvalues of $-\Lambda$ satisfy

$$|\arg(\lambda_i(-\Lambda))| > \frac{\alpha\pi}{2}, \qquad i = 1, 2, 3 \tag{48}$$

Since $\Lambda > 0$, all eigenvalues of $-\Lambda$ lie on the negative real axis. Therefore,

$$|\arg(\lambda_i(-\Lambda))| = \pi > \frac{\alpha\pi}{2}, \qquad 0 < \alpha < 1 \tag{49}$$

Consequently,

$$e(t) \to 0, \qquad t \to \infty \tag{50}$$

For the integer-order case, $\alpha = 1$, and therefore

$${}^{C}D_t^{1} e(t) = \dot{e}(t) \tag{51}$$

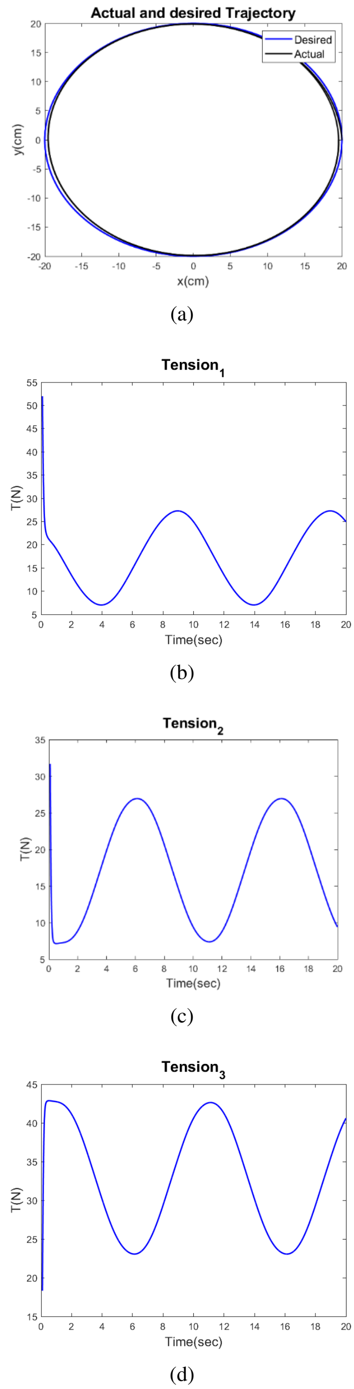

Figure 1. The simulation results for case I.

Hence, the FO sliding surface reduces to

$$s(t) = \dot{e}(t) + \Lambda e(t) \tag{52}$$

Moreover, using

$${}^{C}D_t^{1-\alpha} = {}^{C}D_t^{0} = I \tag{53}$$

the proposed control law reduces to

$$v = \hat{b}^{-1}(X)\left[\ddot{X}_d - \hat{f}(X, \dot{X}) + \Lambda\dot{e} + K_{\rm sm}\,\mathrm{sgn}(s)\right] \tag{54}$$

which corresponds to the conventional integer-order sliding-mode controller.

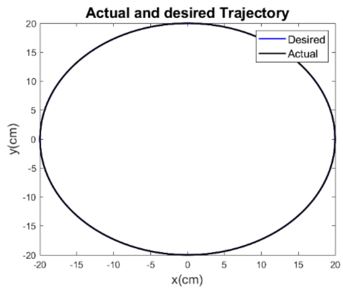

(a)

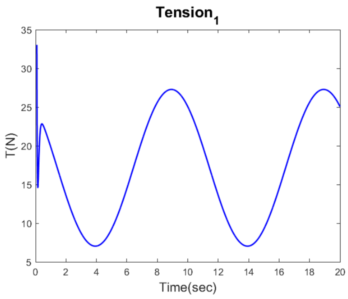

(b)

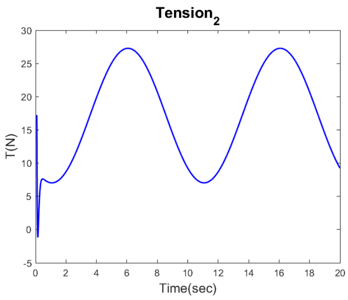

(c)

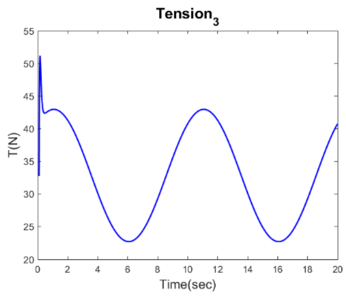

(d)

Figure 2. The simulation results for case II.

IV Results and Simulations

In this section, the simulation is used to show the effectiveness of the proposed method using the MATLAB Simulink. For the CDPR, due to the uncertainty, employing robust control strategies like sliding mode is a necessary consideration. Additionally, given the unstable nature of these robots, implementing a no-chattering controller is crucial. The CDPR's parameters are listed in Tabel 1. In this context, we utilize the FO sliding mode control approach to address this issue. In the previous section, we established two distinct FO values for a circular desired path. Here, we demonstrate the results for two scenarios regarding the values of α with a circular desired path. In the first scenario, the results for an integer-order controller ($\alpha = 1$) are reported for a circular desired path as shown in Fig. 2. In the second scenario, the results for $0 < \alpha < 1$ are demonstrated by setting the FO value $\alpha = 0.8$ considering a circular desired path. The results are shown in Fig. 3. The results indicate that when $0 < \alpha < 1$, the tracking performance surpasses that of the conventional sliding mode. However, determining the optimal value for the order of FO controller remains an open area for research, and this problem can be addressed optimally.

Table 1. The CDPR parameters

Parameters	Symbol	Values
End-effector-mass	m	$3kg$
End-effector-inertial	I_z	$0.2kgm^2$
Gear ratio	N	50
Drum radius	r	$5cm$
Gravity acceleration	g	$9.8m/s^2$

V Conlusion

In this paper, we studied the control problem of CDPR, which involves inherently flexible structures and unavoidable model uncertainties. To mitigate the chattering phenomenon associated with traditional sliding mode control, we adopted a fractional order (FO) modification of this control method. Simulation studies were conducted in MATLAB/Simulink to validate the proposed method. The selection of fractional derivative order remains an open issue; determining its optimal value can be considered a suggestion for future research in this field.

References

[1] Pott A., Bruckmann T. Cable-driven parallel robots. in: *proceedings of the second international conference on cable-driven parallel robots*, Springer, 2014.

[2] Zi B., Qian S. Obstacle avoidance planning of the cooperative cable parallel manipulators for multiple mobile cranes. in: *Design, analysis and control of cable-suspended parallel robots and its applications*, Springer, pp. 233-268, 2017.

[3] Carpio M.A., *et al.* Modeling and oscillations control of a planar parallel robot subsystem activated by cable. in: *IEEE 4th Colombian Conference on Automatic Control*, pp. 1-5, 2019.

[4] Qian S., Zi B., Shang W.W., Xu Q.S. A review on cable-driven parallel robots. *Chinese Journal of Mechanical Engineering*, vol. 31, no. 1, pp. 1-11, 2018.

[5] Abbasnejad G., Tale-Masouleh M. Optimal wrench-closure configuration of spatial reconfigurable cable-driven parallel robots. Proceedings of the Institution of Mechanical Engineers, Part C: *Journal of Mechanical Engineering Science*, vol. 235, no. 19, pp. 4049-4056, 2021.

[6] Alp A.B., Agrawal S.K. Cable suspended robots: feedback controllers with positive inputs. in: *Proceedings of the 2002 American Control Conference*; vol. 1, pp. 815-820, 2002.

[7] Merlet J.P. Some properties of the Irvine cable model and their use for the kinematic analysis of cable-driven parallel robots. *Mechanism and Machine Theory*, vol. 135, pp. 271-280, 2019.

[8] Khosravi M.A., Taghirad H.D. Robust PID control of fully-constrained cable driven parallel robots. *Mechatronics*, vol. 24, no. 2, pp. 87-97, 2014.

[9] Babaghasabha R., Khosravi M.A., Taghirad H. Adaptive robust control of fully-constrained cable driven parallel robots. *Mechatronics*, vol. 25, pp. 27-36, 2015.

[10] Asl H.J., Janabi-Sharifi F. Adaptive neural network control of cable-driven parallel robots with input saturation. *Engineering Applications of Artificial Intelligence*, vol. 65, pp. 252-260, 2017.

[11] Khosravi M.A., Taghirad H.. Experimental performance of robust PID controller on a planar cable robot. in: *Cable-driven parallel robots*, Springer, pp. 337-352, 2012.

[12] Oh S.R., Agrawal SK. Cable suspended planar robots with redundant cables: controllers with positive tensions. *IEEE Transactions on Robotics*, vol. 21, pp. 457-465, 2005.

[13] Katliar M., *et al.* Nonlinear model predictive control of a cable-robot-based motion simulator. *IFAC-PapersOnLine*, vol. 50, pp. 9833-9839, 2017.

[14] Xue R., Ren B., Yan Z., Du Z. A cable-pulley system modeling based position compensation control for a laparoscope surgical robot. *Mechanism and Machine Theory*, vol. 118, pp. 283-299, 2017.

[15] Bayani H., Masouleh M.T., Kalhor A. An experimental study on the vision-based control and identification of planar cable-driven parallel robots. *Robotics and Autonomous Systems*, vol. 75, pp. 187-202, 2016.

[16] Gholipour R., Khosravi A., Shokoohinia M.R. Adaptive disturbance rejection sliding mode control for robots via an orthogonal functions-based estimator. *International Journal of Industrial Electronics Control and Optimization*, 10.22111/ieco.2026.53699.1726, 2026.

[17] Korayem M.H., Taherifar M., Tourajizadeh H. Compensating the flexibility uncertainties of a cable suspended robot using SMC approach. *Robotica*, vol. 33, pp. 578-598, 2015.

[18] Gholipour R., Fateh M.M. Designing a robust control scheme for robotic systems with an adaptive observer. International Journal of Engineering 2019.

[19] Gholipour R., Fateh M.M. Adaptive task-space control of robot manipulators using the Fourier series expansion without task-space velocity measurements. *Measurement*, vol. 123, pp. 285-292, 2018.

[20] Baklouti S., Courteille E., Lemoine P., Caro S. Vibration reduction of cable-driven parallel robots through elastodynamic model-based control. *Mechanism and Machine Theory*, vol. 139, pp. 329-345, 2019.

[21] Abedi Pahnehkolaei S.M., Alfi, A., Machado, J.T. Stabilization of fractional-order systems subject to saturation element using fractional dynamic output feedback sliding mode control. *Computational and Applied Mathematics*, vol. 12, p. 031014, 2017.

[22] Abedi Pahnehkolaei S.M., Alfi, A., Machado, J.T. Fuzzy logic embedding of fractional order sliding mode and state feedback controllers for synchronization of uncertain fractional chaotic systems. *Computational and Applied Mathematics*, vol. 39, no. 3, p. 182, 2020.

[23] Khosravi, M., Taghirad, H. Experimental performance of robust PID controller on a planar cable robot. *Cable-Driven Parallel Robots*, pp. 337–352, Springer, 2012.

[24] Sabatier, J.A., Agrawal, O.P., Machado, J.T. *Advances in fractional calculus*, Dordrecht: Springer, 2007.